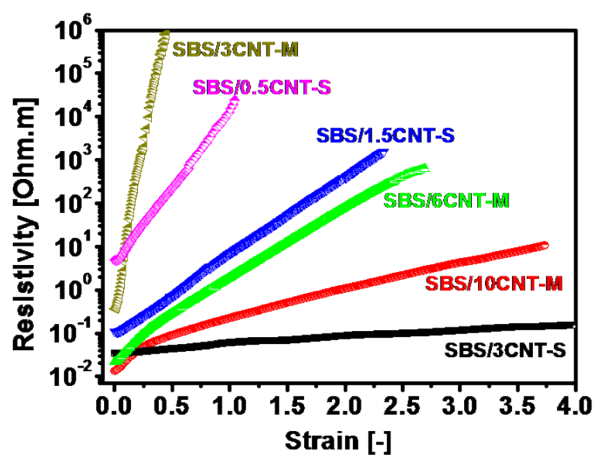
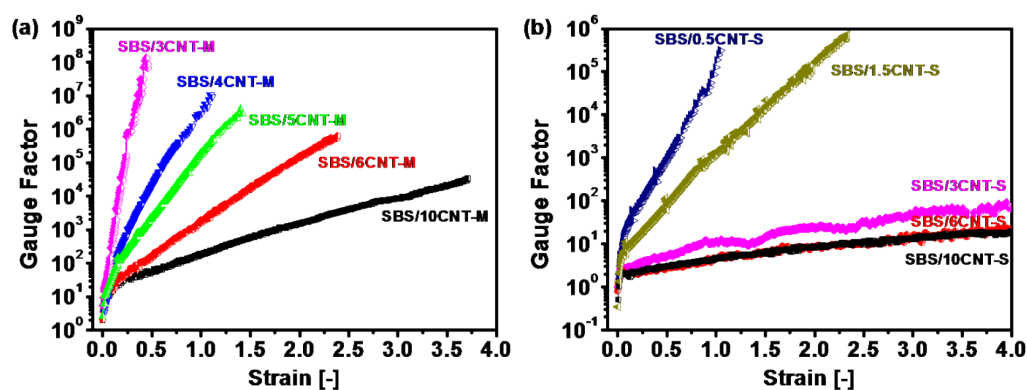


## Supporting Information



**Fig. S1** Strain sensing behavior comparison of some composites with similar initial conductivity.



**Fig. S2** Gauge factor as a function of strain for SBS/MWCNT composites fabricated by melt processing (a), and solution casting (b).

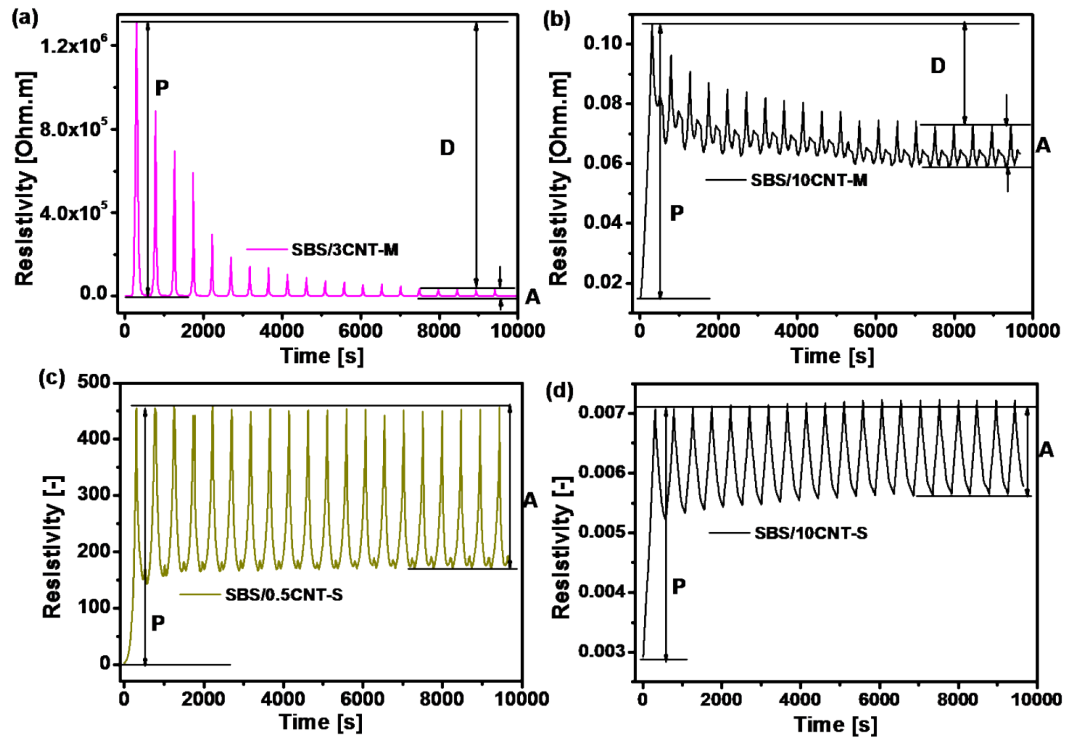


**Fig. S3** The electrical resistivity evolution under dynamic strain cycles (20 cycles at a strain between 0.1~0.5) for (a) SBS/3CNT-M; (b) SBS/10CNT-M; (c) SBS/0.5CNT-S; and (d) SBS/10CNT-S.

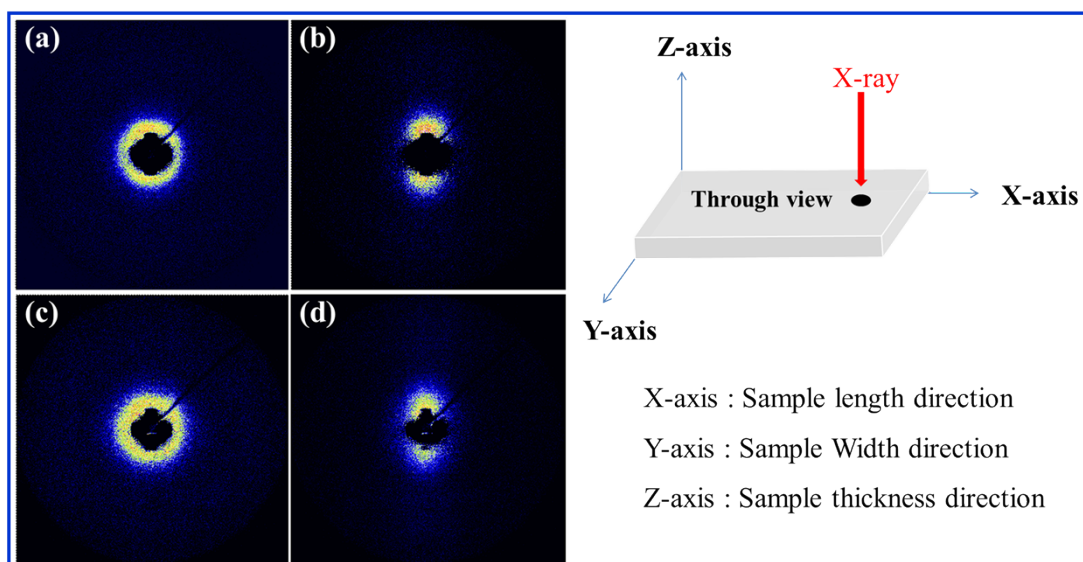


**Fig. S4** 2D SAXS pattern corresponding to (a) SBS/10CNT-M under zero-strain; (b) SBS/10CNT-M under 200% strain; (c) SBS/10CNT-S under zero-strain; and (d) SBS/10CNT-S under 200% strain. And a schematic diagram of X-ray beam direction relative to samples is on the right.

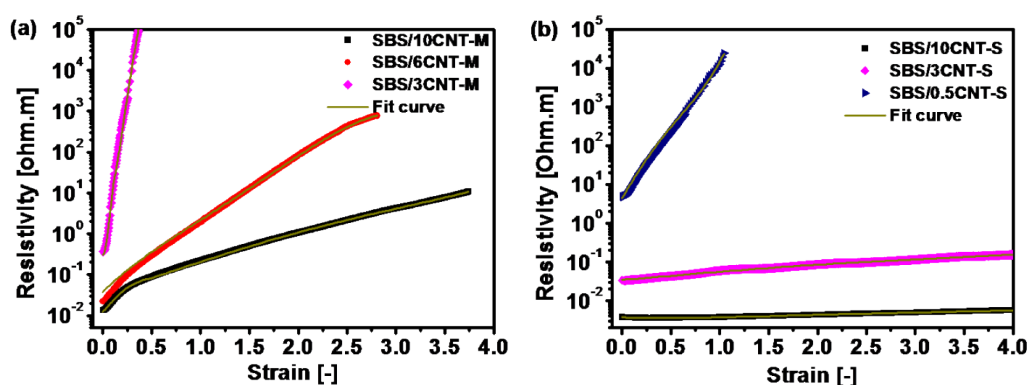


**Fig. S5** Experimental (dots), theoretical (dark yellow) data of strain-dependent resistivity change for SBS/MWCNT composites fabricated by melt processing (a), and solution casting (b).

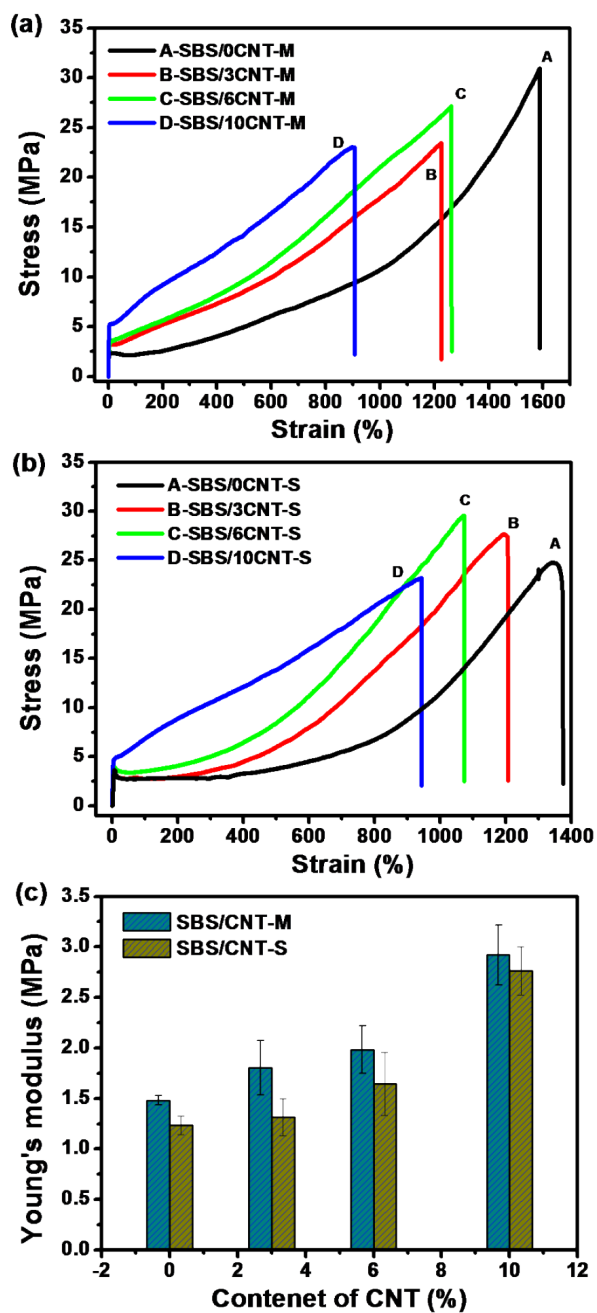


**Fig. S6** The typical stress-strain curves of SBS/MWCNT composites fabricated by melt processing (a), and solution casting (b); (c) Young's modulus comparison of the above composites.

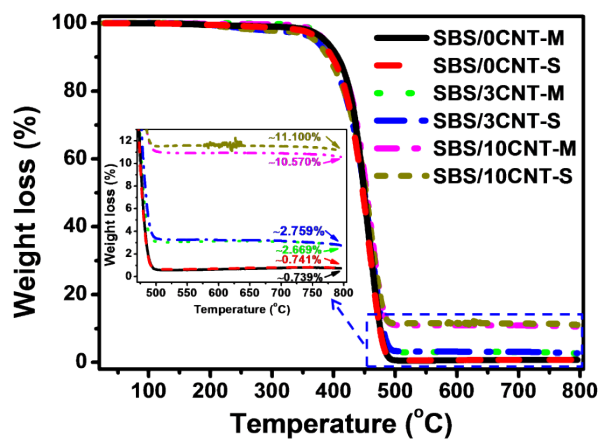


**Fig. S7** Thermogravimetric curves for SBS/MWCNT composites with various contents of MWCNT fabricated by melt processing and solution casting with insert of an expansion of curves.

**Tab. S1** The recovery ratio of conductive network during dynamic stretching and amplitude of resistivity peak shown in Fig. S4.

	SBS/3CNT-M	SBS/0.5CNT-S	SBS/10CNT-M	SBS/10CNT-S
D/P	97%	0	37%	0
A	776.787	280.029	0.013	0.002